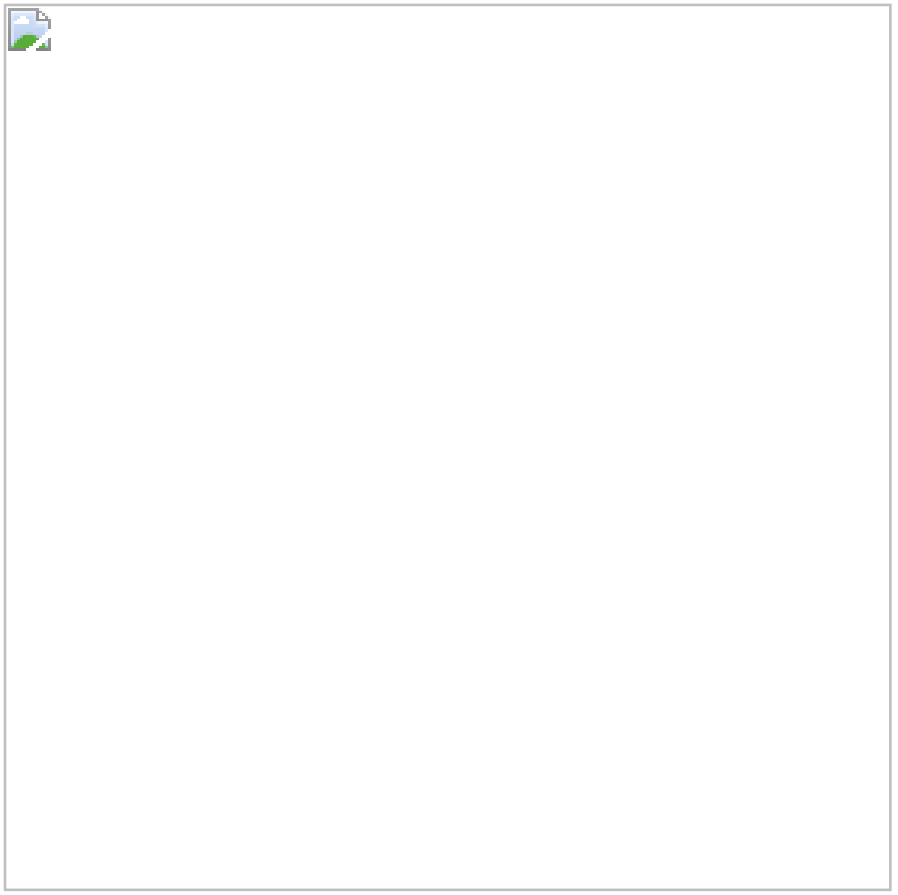

Risk of Surface Sediment Erosion in the Bohai Sea, North Yellow Sea and Its Indication to Tidal Sand Ridge Occurrence

Authors: Tang, Cheng, Li, Yanfang, Liu, Xin, Zhao, Yan, and Zhang, Hua

Source: Journal of Coastal Research, 74(sp1) : 126-135

Published By: Coastal Education and Research Foundation

URL: https://doi.org/10.2112/SI74-012.1

Journal of Coastal Research	SI	74	126–135	Coconut Creek, Florida	2016

Risk of Surface Sediment Erosion in the Bohai Sea, North Yellow Sea and Its Indication to Tidal Sand Ridge Occurrence

Cheng Tang[‡*], Yanfang Li[‡], Xin Liu[‡], Yan Zhao[‡], and Hua Zhang[‡]

[‡] Yantai Institute of Coastal Zone Research
Chinese Academy of Sciences
Yantai, Shandong 264003, P. R. China

www. cerf-jcr. org

www. JCRonline. org

ABSTRACT

Tang, C.; Li, Y. F.; Liu, X.; Zhao, Y., and Zhang, H., 2016. Risk of surface sediment erosion in the Bohai Sea, North Yellow Sea and its indication to tidal sand ridge occurrence. *In*: Harff, J. and Zhang, H. (eds.), *Environmental Processes and the Natural and Anthropogenic Forcing in the Bohai Sea, Eastern Asia. Journal of Coastal Research*, Special Issue, No. 74, pp. 126–135. Coconut Creek (Florida), ISSN 0749–0208.

Bottom geomorphological evolution and sediment distribution are under strong control of tidal forcing along China's coast. To quantify and assess the temporal-spatial change of bottom environment, a risk-based probabilistic concept of erosion is applied and maps of erosion risk are constructed. Sediment data categorized into 5 classes, together with hydrodynamic data in a temporal resolution of one hour and a model time of one month, are used to calculate the potential of erosion of surface sediments in the Bohai Sea, North Yellow Sea. Comparison with results of the tidal ellipse and bottom shear stress from model output shows that the highest risk of erosion is located in the Yalujiang Estuary, West Korea Bay, north of the Bohai Bay and in the surroundings of the Laotieshan channel of Bohai Strait, which may explain the occurrence of tidal sand ridges in the modeling domain.

ADDITIONAL INDEX WORDS: *Tidal sand ridge, erosion risk analysis, Bohai Sea, North Yellow Sea.*

INTRODUCTION

Sediment dynamics play an important role in forming the bottom geomorphology and affecting the sediment distribution in coastal waters. More and more coastal engineering projects like offshore construction or seabed pipeline routing request to estimate the potential of erosion on the seafloor bottom surface, to investigate the occurrence of special bottom morphology, *e.g.* tidal sand ridge distribution and development along Chinese coasts (Liu *et al.*, 1998; Swift, 1975; Wang *et al.*, 2012; Yang, 1989). Considering the variety of bottom sediment types and specific sediment distribution patterns, a methodology of assessing and quantifying the status of bottom dynamics is required, studying the natural dynamics of surface sediment and its interaction with human activities.

Threshold value is a widely used tool for description of bottom erosion status. Belderson (1986) found that mean spring near-surface peak tidal currents exceeding 0.5 m/s are responsible for the formation of sand waves in the North Sea, providing evidence that the magnitude of tidal currents and the occurrence of sand waves are related. To overcome the difficulty in getting reliable values of critical shear stress/velocity for the initial sediment motion and suspension, Grass (1970) demonstrated the need to use statistical tools to improve the evaluation of sediment-motion processes. Lopez and Garcia (2001) later developed this idea into a risk-based probabilistic approach; they used basic probability tools in characterization of the turbulent processes involved in the mechanics of sediment transport. This method was first applied to analyze the surface erosion risk of Mecklenburg Bight in the Baltic Sea (Bohling, 2005) where sediment characteristics and critical shear stress velocities were used to calculate the risk of sediment erosion.

In this research, we use the concept "Erosion Risk" instead of kind of threshold initial value of sediment motion to assess the bottom environment in the Bohai Sea, North Yellow Sea (BSNYS; Figure 1). BSNYS is a semi-closed shallow shelf sea, affected by the dynamic processes of tides, waves and regional currents. It receives large amounts of sediment from many rivers in China, for instance the Yellow River, and rivers from Korea (Park and Lee, 1994). The sea bottom is mostly flat and water depth less than 100 meters. The area is largely dominated by mixed semi-diurnal tidal regime, with tidal range exceeding 4 m in many coastal regions. Seasonal current patterns develop in the Yellow Sea affected by monsoonal winds. In Summer, the primary circulation in this region is characterized by NYSCW (Northern Yellow Sea Cold Water), which is anticlockwise induced by the sea-surface heating and vertical mixing of the tidal currents and bottom topography, in winter by the northernward YSWC (Yellow Sea Warm Current) and CC (Coastal Current) (Lu *et al.*, 2011; Shi *et al.*, 2012). Sediment at the seafloor and the hydrodynamic modeling data were gathered in a Geological Information System (GIS). Bottom erosion status indexed by erosion risk is

DOI: *10. 2112/SI74–012. 1 received* (*2 February 2015*); *accepted in revision* (*23 December 2015*).

*Corresponding author; ctang@ yic. ac. cn

calculated based on these data. Four sites were selected to assess the temporal and spatial change of erosion risk in the study domain, the relationship between the erosion risk distribution and the occurrence of tidal sand ridge is discussed in the final section.

DATA SET

Sediment data

Surface sediments characteristics used in this study were mainly adopted from a sediment distribution map published by Li *et al.* (2005) and other sources (Park and Lee, 1994; Shi *et al.*, 2012; Zhu and Chang, 2000). 18 sediment types (Figure 2) using Shepard (1954) classification method were digitized into the ARCGIS database. Following the concept of "regionalized classification" (Harff and Davis, 1990), these sediments types were categorized into 5 subclasses (see Table 1, Figure 2) with reference to Bobertz and Harff (2004), Bohling (2005), Rijn (2007). Silt is primarily distributed in the coastal area of Bohai Sea with more than 80% silt content by weight, badly sorted, and with mean size of 5.5 φ (Shi *et al.*, 2012). Clayey silt is one of the most widely distributed sediments inside the Bohai Sea and center of north Yellow Sea, with 60% of silt, about 2% by sand and 38% of clay, the mean grain size is 7.5 φ (Shi *et al.*, 2012; Zhu and Chang, 2000). These 2 types of sediments belong to cohesive sediment, where the threshold value of critical shear stress is hard to be observed. Here, the value of critical shear stress is adopted from Rijn (2007). He showed that for sediment bed with size in the range of 8–62 μm corresponding to an approximately constant shear stress value of 0.1 N/m^2, will result in a critical depth-average current velocity of about 0.32 m/s. Critical shears stress of 0.2 N/m^2 will result in a critical depth-averaged current velocity of about 0.42 m/s with D50 < 62 μm. To simplify the classification process, 2 types of cohesive sediment were distinguished based on the literature research (Table 1). Coarse-fine silt represent the cohesive-weakly cohesive sediment which most distribute along the coastal waters of Bohai Sea (Figure 3), while clayey silt and very fine silt represent the very cohesive type which covered most area of the Bohai Sea and west part of the Yellow Sea.

The sandy sediments are subdivided into 3 classes although previous studies put them all in one class (Shi *et al.*, 2012; Zhu and Chang, 2000). Sand dominantly occurs in the northeast Yellow Sea, along the Laotieshan channel in the Bohai Strait. It is believed that these sandy sediments are formed after the postglacial transgression maximum by strong tidal currents and subsequent shelf erosion (Dong *et al.*, 1989; Li *et al.*, 2001). Since lack of laboratory experimental observation data for the critical shear stress/velocity in this region, the critical erosion stress for noncohesive sediment is based on the Sediment-Transport Applets from USGS (http://woodshole.er.usgs.gov/staffpages/csherwood/sedx_equations/RunSedCalcs.html). The mean velocity calculated from critical shear stress is referred to the formula derived by Prof. Ponce (http://ponce.sdsu.edu/critical_shear_stress_versus_critical_velocity.html).

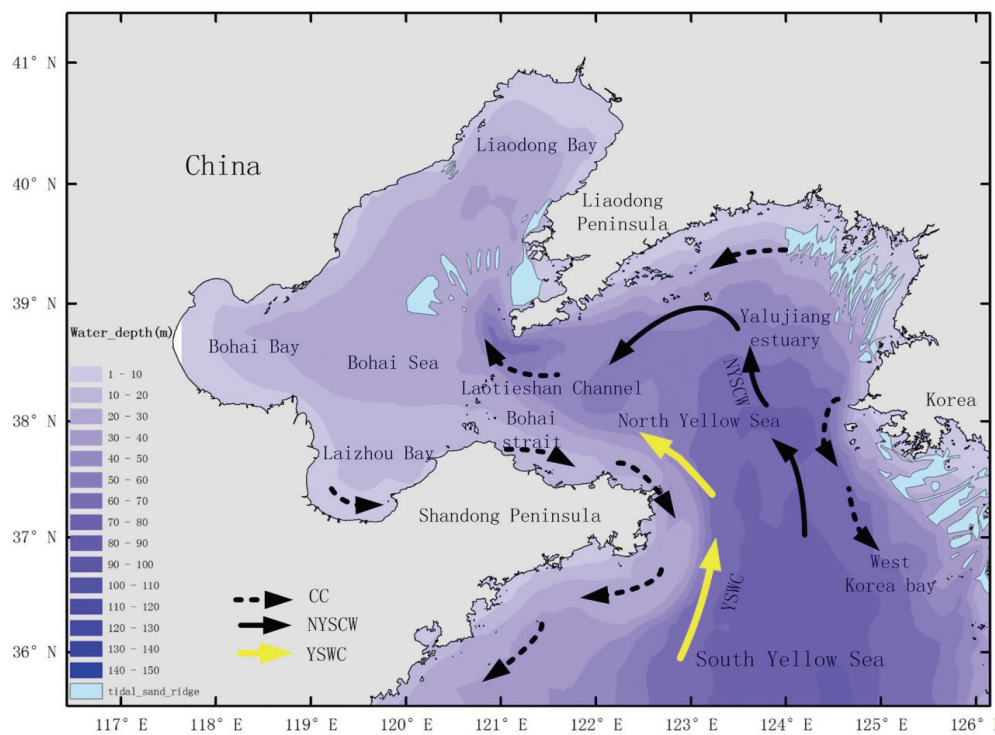

Figure 1. The study area with tidal sand ridges with schematic pattern of the regional circulation in BSNYS in summer, NYSCW (Northern Yellow Sea Cold Water), and in winter, YSWC (Yellow Sea Warm Current). CC: Coastal Current (circulation pattern adopted from Shi *et al.*, 2012, sand ridge distribution from Wang *et al.*, 2012)

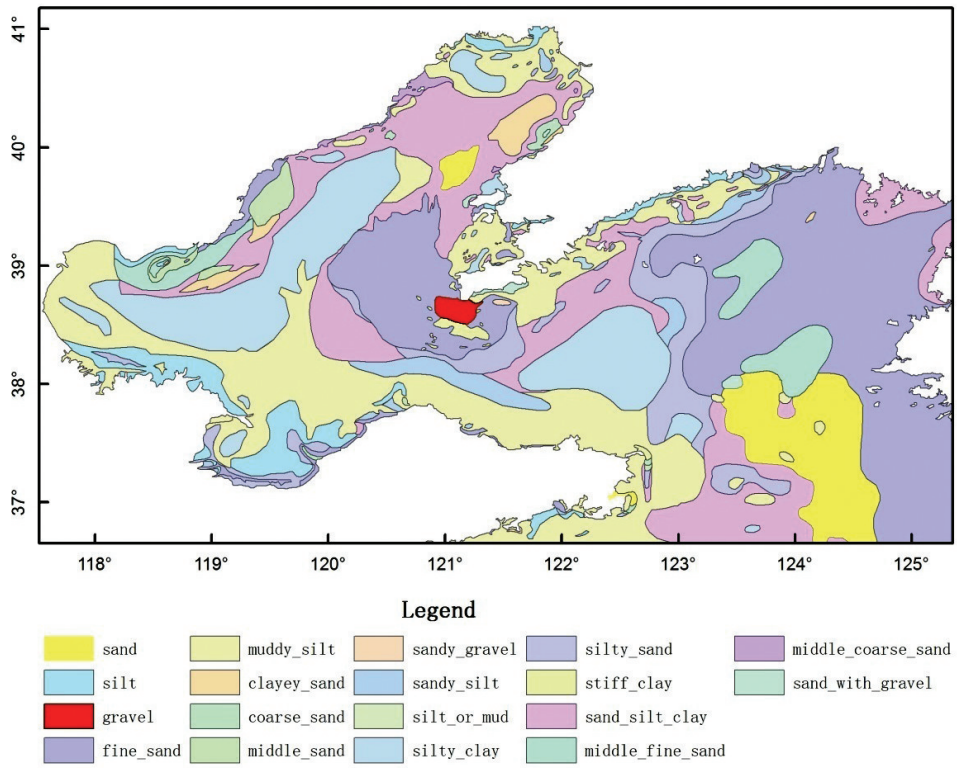

Figure 2. The digitized sediment distribution map based on Li *et al*., 2005

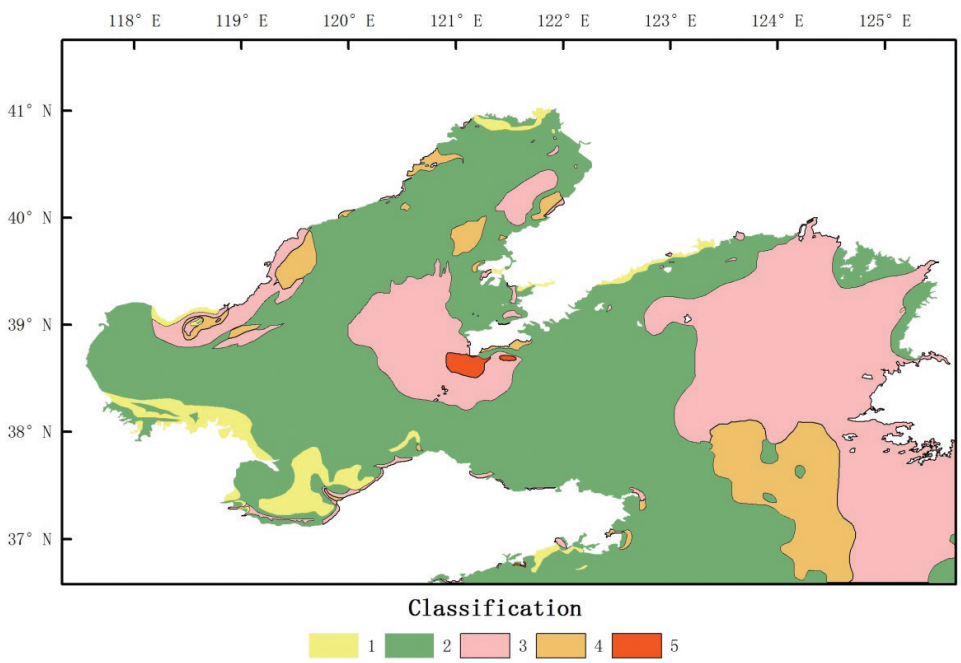

Figure 3. The re-classified sediment distribution map of Bohai Sea, north Yellow Sea, 5 sediment types' characteristic see Table 1

Table 1. *The corresponding properties of* 5 *sediment classes used in bottom sediment erosion risk model*

Nr.	Sediment type	Grain size (φ)	Grain size (um)	Critical erosion stress (N/m^2)	mean velocity (m/s)	Deviation of mean velocity
1	Coarse – fine silt (cohesive-weakly cohesive)	4–8	8–62	0.1	0.32	–
2	Clayey silt, very fine silt (very cohesive)	4–8	8–62	0.2	0.42	–
3	Fine sand (noncohesive)	3–4	62–125	0.0943–0.137	0.217–0.262	0.3
4	Medium sand (noncohesive)	2–3	125–250	0.137– 0.191	0.262–0.309	0.3
5	Coarse sand–gravel(noncohesive)	1–2	250–500	0.191–0.278	0.309–0.373	0.4

Hydrodynamic data

The hydrodynamic data are model output from Regional Ocean Modeling System (ROMS), which is a free-surface, terrain-following, primitive equations model using the hydrostatic and Boussinesq assumptions. The model domain covers the Bohai Sea, North Yellow Sea with a 5 km resolution in latitude and longitude, and with 20 layers in the vertical resolution. The time-step used for the three-dimensional baroclinic model is 300 s. The bathymetry of the model is interpolated from digitized nautical charts and ETOPO1 data set. 6 hourly forcing from NCEP reanalysis data of heat flux, wind stress are used for the model bulk driving force. The four principal and most common used tidal harmonic constituent M2, S2, K1 and O1 are applied as tidal forcing in the model, and the tidal data are derived from the suite of global and regional tide model TPXO8 dataset. For the lateral open boundaries, horizontal sea water velocity and sea surface elevation are specified from climatologically potential temperature and salinity assembled from the World Ocean Atlas 2005 (WOA05) data set. The model is initialized on 1 December, 2011 from a state of rest with the temperature and salinity specified from the WOA05, and set to run one year (2012) in this study.

The wave forcing data are derived by running the Simulating WAves Nearshore (SWAN) model offline. The SWAN model uses 6 hourly wind derived data from the NCEP reanalysis data to calculate the wind-induced wave height, wave direction, and bottom wave period in the modeling domain. The SSW-BBL bottom boundary layer module is used in the numerical computation. These wave data are used to calculate the near-bed velocity and the wave-current shear stresses which have influence on sediment suspension/deposition.

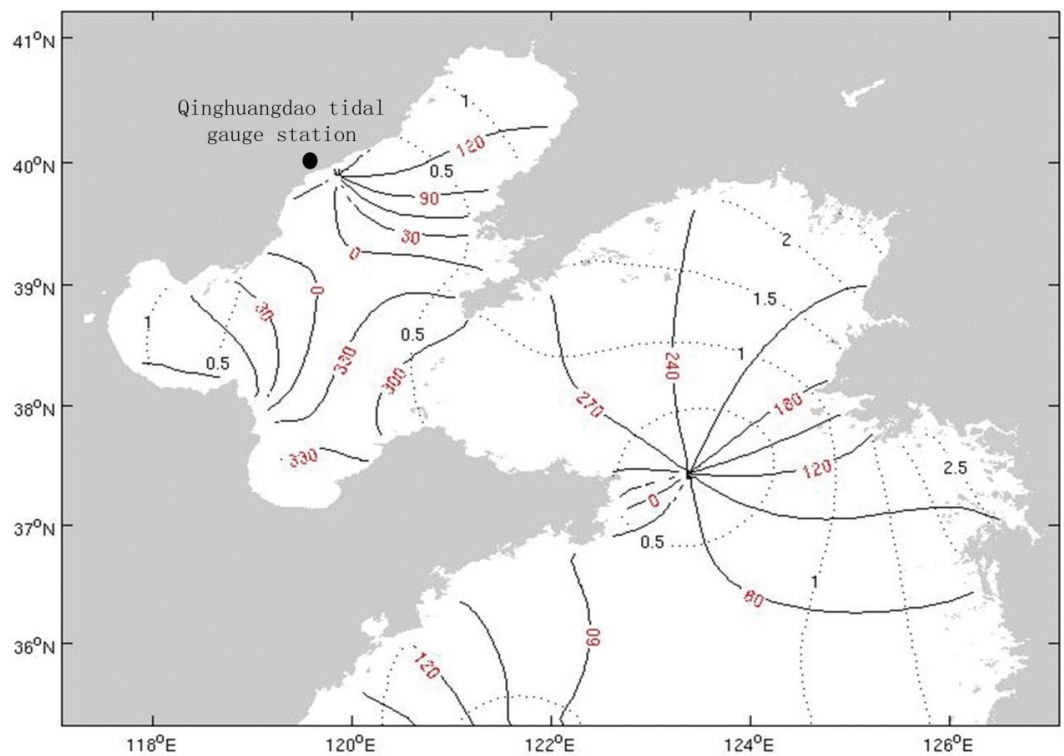

Figure 4. The co-tidal chart of M2 constituent from the numerical model. Solid line: phase-lag (in deg.), dashed line: amplitude (in m)

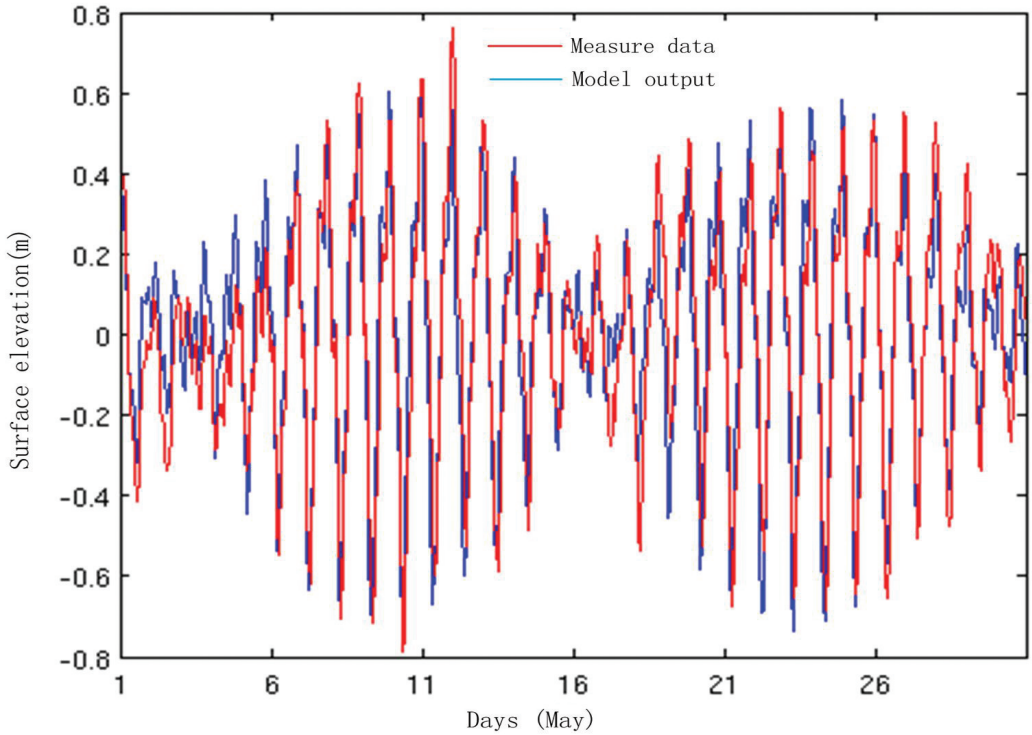

Figure 5. Time series comparing measured tides (red line) and model output (blue line) at the tidal gauge station Qinghuangdao (black dot marked in Figure 4), the correlation index is 0.9

The modeled sea surface elevation results are used to calculate the harmonic constants of the tidal constituents in order to validate the model. The co-tidal and co-amplitude lines of the M2 tide, which are the dominant diurnal constituents in the Bohai Sea, North Yellow Sea, generated by the model in the BSNYS are shown in Figure 4. This structure agrees with the previous works (Bian *et al.*, 2013; Fang *et al.*, 2004; Lu *et al.*, 2011; Xia *et al.*, 2006). Sea surface elevation time-series from the model output compared with the tidal gauge measurement in May in Qinghuangdao station is shown in Figure 5, and the average correlation between modeled and observed tides is 0.9. The results show that the simulated tide agrees well with the observations.

METHODS

The dynamics of the bottom boundary layer (BBL) which provide the information of hydrodynamic process by near bottom flows and waves near the seabed in a short vertical distance are well studied in coastal waters (Grant and Madsen, 1979; Jonsson and Carlsen, 1976; Madsen, 1994; Smith, 1977; Styles and Glenn, 2000). The bottom shear stress generated in the BBL plays the main role in sediment transport (Fredsoe and Deigaard, 1992; Kuhrts *et al.*, 2004; Soulsby, 1997). If the bottom shear stress exceeds the critical values for bed load transport or resuspension, the sediment is mobilized from the seabed. On the contrary, when the shear stress falls below a critical value, the suspended sediment will settle.

Due to the fact that the sediment erosion takes place gradually over a wide range of shear stress velocities as the flow velocity is increasing (Grass, 1970), the idea of using stochastic method to describe the nature of the sediment erosion was developed (Lavelle and Mofjeld, 1987). Based on the assumption that the erosion risk is equal to the probability and its distribution follow Gaussian normal distribution, Lopez and Garcia (2001) developed a risk-based probabilistic approach using polynomial approximation. The erosion risk Ri can be estimated as:

$$\text{if } \frac{\bar{\tau}_c - \bar{\tau}_f}{\sqrt{\sigma_c^2 + \sigma_f^2}} < 0,$$

$$Ri = \frac{1}{2}\left[1 + a_1\left|\frac{\bar{\tau}_c - \bar{\tau}_f}{\sqrt{\sigma_c^2 + \sigma_f^2}}\right| + a_2\left|\frac{\bar{\tau}_c - \bar{\tau}_f}{\sqrt{\sigma_c^2 + \sigma_f^2}}\right|^2 + a_3\left|\frac{\bar{\tau}_c - \bar{\tau}_f}{\sqrt{\sigma_c^2 + \sigma_f^2}}\right|^3 + a_4\left|\frac{\bar{\tau}_c - \bar{\tau}_f}{\sqrt{\sigma_c^2 + \sigma_f^2}}\right|^4\right] \quad (1)$$

$$\text{and if } \frac{\bar{\tau}_c - \bar{\tau}_f}{\sqrt{\sigma_c^2 + \sigma_f^2}} \geqslant 0$$

$$Ri = 1 - \frac{1}{2}\left[1 + a_1\left|\frac{\bar{\tau}_c - \bar{\tau}_f}{\sqrt{\sigma_c^2 + \sigma_f^2}}\right| + a_2\left|\frac{\bar{\tau}_c - \bar{\tau}_f}{\sqrt{\sigma_c^2 + \sigma_f^2}}\right|^2 + a_3\left|\frac{\bar{\tau}_c - \bar{\tau}_f}{\sqrt{\sigma_c^2 + \sigma_f^2}}\right|^3 + a_4\left|\frac{\bar{\tau}_c - \bar{\tau}_f}{\sqrt{\sigma_c^2 + \sigma_f^2}}\right|^4\right] \quad (2)$$

Here, $a_1 = 0.196854$, $a_2 = 0.115194$, $a_3 = 0.000344$, a_4

= 0.019527, $\bar{\tau}_c$, $\bar{\tau}_f$ represent the resistance and the loading force for the initial state of the sediment, and σ_c, σ_f is the standard deviation of the two forces mentioned above. To calculate the risk of erosion, we use an approximate methodology here, $\bar{\tau}_c$ is the mean shear stress velocity derived from the critical shear stress (Table. 1) (m/s), $\bar{\tau}_f$ is the mean flow-wave velocity above the seabed from the model output (m/s), σ_c is the standard deviation of critical shear stress velocity (m/s) with reference to the method of Bohling (2005), and σ_f is the standard deviation of flow-wave induced velocity (m/s). To estimate the variability of the instantaneous flow- and wave- induced shear stress velocity, we use $\sigma_f = 0.4\bar{\tau}_f$, this follows the approach by Grass (1970), which was also applied by Lopez and Gacia (2001), and Bohling (2005). By using the GIS spatial analysis, all data sets including the sedimentologic and hydrodynamic data were interpolated at the same grid. The erosion risk is calculated on every grid point with different time slot data.

RESULTS

As the hydrodynamic model uses climatological reanalysis of wind data as a driving force, the low temporal resolution output cannot resolve for the calculation of strong storm events, which normally last for short time but produce significant bottom erosion risk. Here, our main concern is the bottom environment under long term forcing. A mean erosion risk distribution map is made based on the calculation of one month hour by hour model output (Figure 6). Seven erosion risk zones (A–G) can be recognized referring to the erosion risk index. The Yalujiang Estuary (A), West of Korea Bay (B), northern area of the Bohai Bay (G) and surroundings of Laotieshan Channel in the northern part of Bohai Strait (C) show significant high values, and their corresponding sediment types are mostly sand. The eastern waters of Shandong Peninsula (D) show a relative high risk value compared to that of zones A, B, C. In the north-east of Liaodong Bay, Zone E has mostly the fine sand at sea bottom, and also shows a comparative medium value. Zone F is located in the west of Liaodong Bay, and the erosion risk distribution has a similar erosion risk pattern, showing slightly higher values compared to surrounding areas. As sediment transport takes place when a certain critical shear stress is exceeded, the same pattern can be found in the bottom shear stress distribution from model output (Figure 7). Since wave induced bottom shear stress is large where water depth is less than 10 m, and almost zero where water depth is more than 20 m (Figure 8), it can be shown that the mean erosion risk is strongly related to bottom shear stress induced by the current.

4 sites representing 4 typical sedimentation areas in the BSNYS (T1, T2, T3 and T4 in Figure 6) were selected to check the erosion risk status through one month of simulation (Figure 9), and the time serials of each pattern follows the track of tidal cycle. T1 is close to the central part of Bohai Sea, where the circulation in the Bohai Sea is relatively weak (Lu *et al.*, 2011), and its erosion risk index in one tidal cycle generally less than 0.5, the average value is 0.1568. T2 is located in the west part of the Laotieshan water channel, where small elongated tidal sand ridges exist in the surrounding area (Wang *et al.*, 2012). Affected by the strong current through the tidal channel, its risk index can up to 0.9 during the strong tidal force, and the mean value is 0.5019. T3 is in the east part of Shandong Peninsula, close to the central of north Yellow Sea, affected by different seasonal circulation, and the erosion risk varied during the whole tidal period with a mean value of 0.3744. T4 is located in the western part of Korea Bay, where the best development of tidal-current ridges can be found at bay-heads (Chough *et al.*, 2002), and it is also the place where the strong tide current play a role. The erosion risk is all the way in a high value (up to 0.9) and its average value is 0.7285.

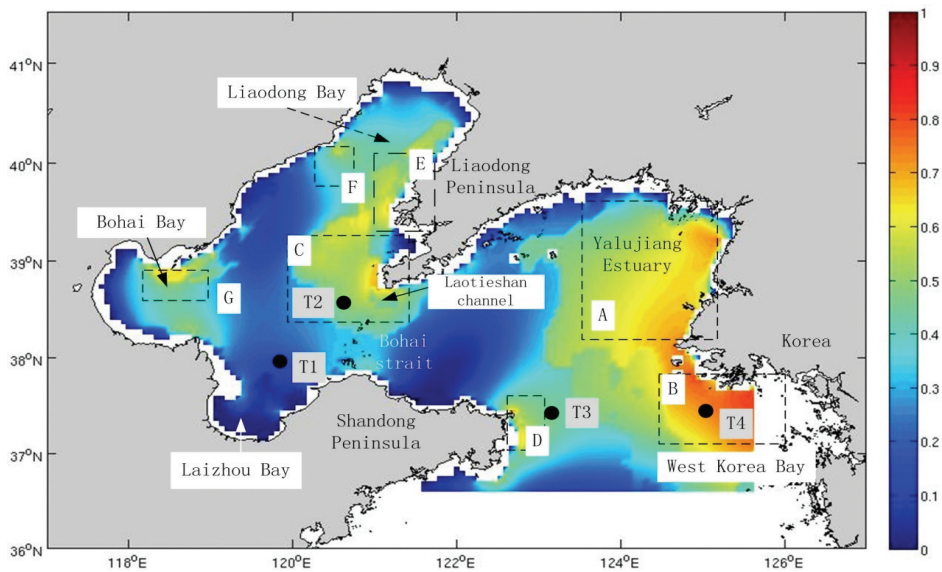

Figure 6. The average erosion risk distribution in the study area with seven risk zones (A–G), the colors in the study domain represent the erosion index from 0 to 1

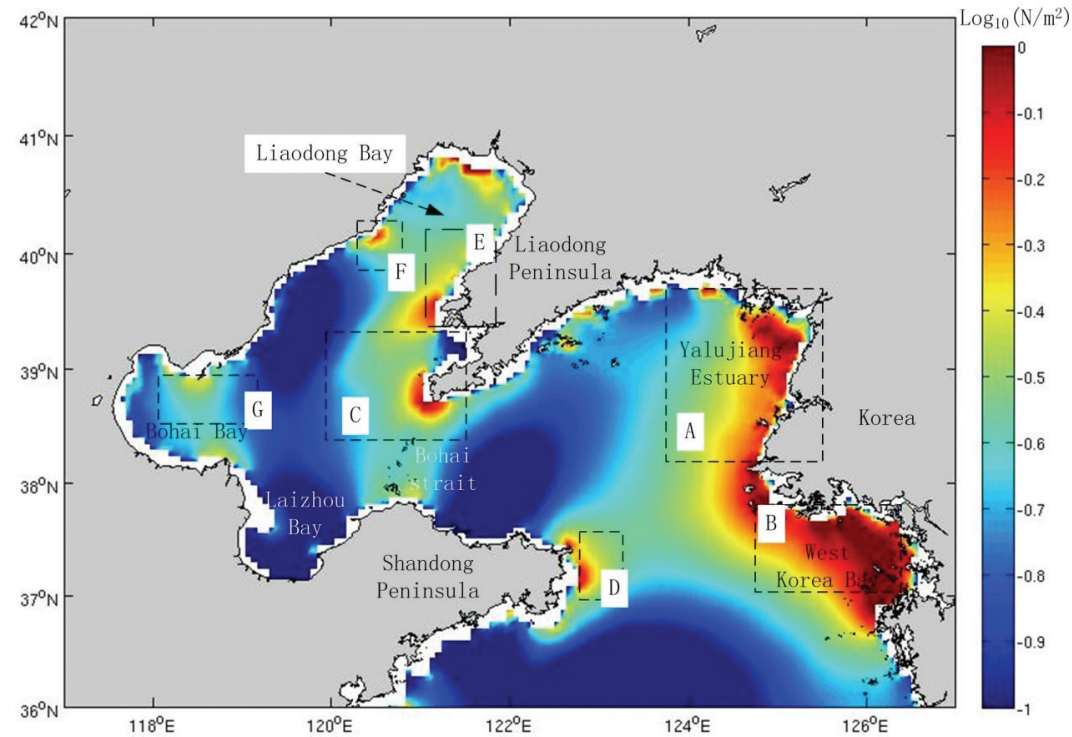

Figure 7. Bottomshear-stress distribution induced by currents and waves from model output

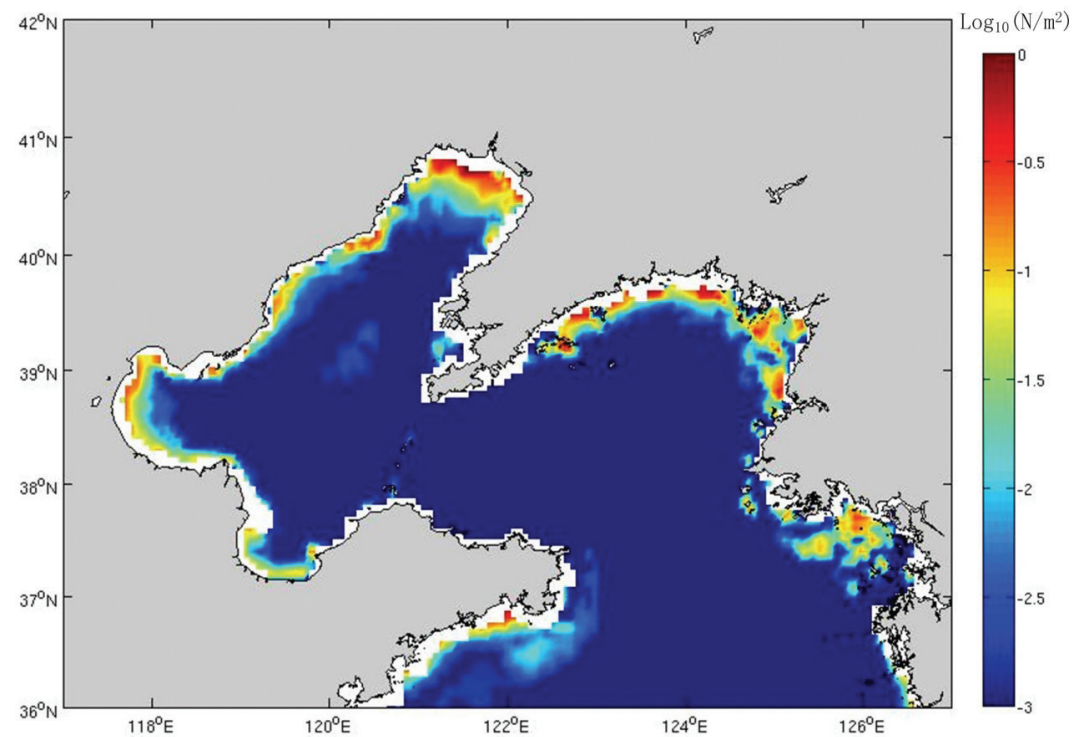

Figure 8. Bottomshear-stress caused by waves from the model output

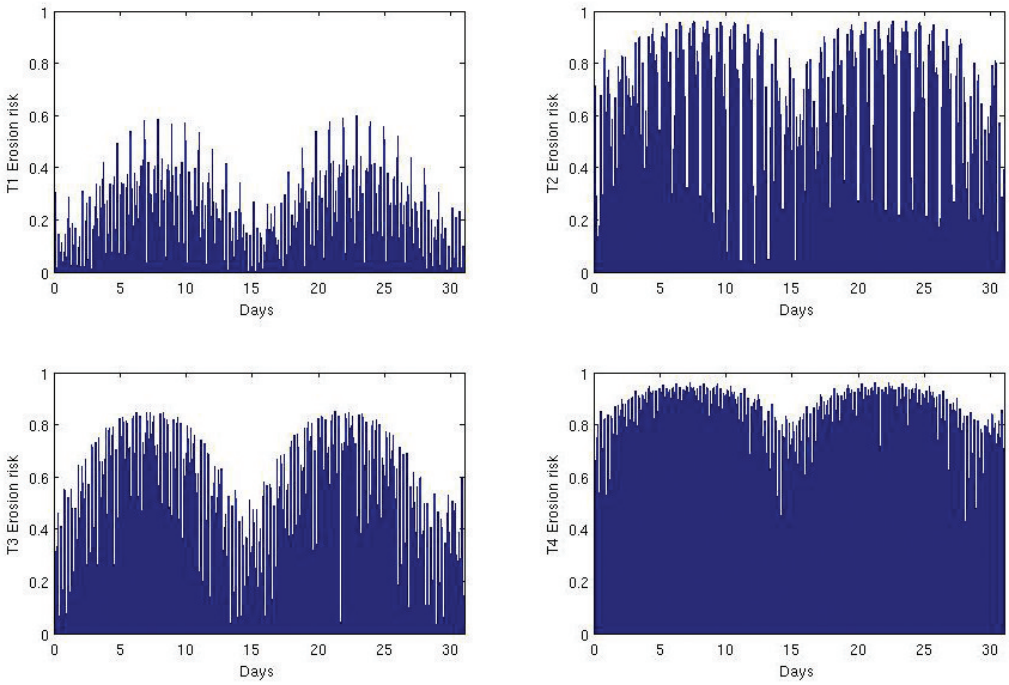

Figure 9. The erosion risk histogram chart of 4 specific locations in the modeling domain

DISCUSSION

Sand ridge occurrence indicated by erosion risk

Tidal sand ridges may develop if the tidal currents meet the criteria favorable for sand ridge formation (Yang, 1989; Uehara *et al.*, 2002). Liu *et al.* (1998) suggested a critical tidal current speed of 150 cm/s for the accretion of shallow ridges and coast tidal flats. The crests orientation of the sand ridge is parallel to the prevailing tidal current (Hulscher & Brink, 2001). To elaborate the bottom dynamic environment where the sand ridges exist, the erosion risk index might be a good indicator together with other factors, like pre-existing morphology, river discharge and storm wave process and so on. In our case, the average erosion risk-index above 0.5 shows a strong hydraulic regime with tidal ridge existence. In the previous study, the tidal sand ridges existing in the zone A, B, C, E, F have been widely cited (Figure 1, Chough *et al.*, 2002; Li *et al.*, 2001; Liu et al, 1998; Park & Lee, 1994; Wang *et al.*, 2012). The recent discovered sand ridges in the Bohai Sea (Wang *et al.*, 2006; Wang *et al.*, 2015) which are in the corresponding zone D and G in the research domain give a good proof that erosion risk might be a good clue in looking for the potential location of sand ridge.

Sediment distribution patterns

The high erosion risk generally represents the high dynamic situation. A numerical simulation of tidal elevations and currents in the Bohai Sea and East China Sea shows that the erosion/accretion patterns of sediments with different grain size are determined by differences in the sediment transport rate (Zhu and Chang, 2000). The strong currents rework the area where sand ridges exist, and fine sediments are transported seawards by the tidal current. This may explain that the occurrence of high erosion risk has a close connection with the occurrence of sand at the sea bottom, and detailed database of sediment distribution is essential in such studies (Veen *et al.*, 2006). The exact link between bottom sediment and erosion risk is not completely secure so far, although in the paper we calculated erosion risk related to both cohesive and non-cohesive sediments and presented the its distribution of the Bohai Sea for a whole picture. More work on modeling the erosion process especially related to cohesive sediments need to be done in the future.

SUMMARY AND CONCLUSION

Estimation of erosion risk can be a helpful indicator to describe the bottom dynamic conditions of the Bohai Sea, North Yellow Sea. Seven areas of high erosion risk were recognized from average erosion risk distribution, which is based on the risk calculation from hydrodynamic model output and GIS sedimentary database. The seven zones fit well with the occurrence of tidal sand ridges from literature findings. It has been found that areas with mean erosion risk above 0.5 correspond directly to the tidal sand ridge environment. More experimental information is required to accurately determine the erosion risk for different sediment characteristics and flow conditions. The model is a good starting point to investigate the occurrence of large-scale morphological features.

ACKNOWLEDGEMENT

This study is jointly supported by the funds numbered with KZZD-EW-14 from Chinese Academy of Sciences, 2015CB453300 from

National Basic Research Program of China (973), and 41530966, 41371483, 41006055 from National Natural Science Foundation of China.

LITERATURE CITED

Belderson, R. H., 1986. Offshore tidal and non-tidal sand ridges and sheets: differences in morphology and hydrodynamic setting. In: Knight, R. J.; McLean, J. R. (eds.), Shelf sands and sandstones. *Canadian Society of Petroleum Geologists Memoir*, 11, 293-301.

Bian, C.; Jiang, W., and Greatbatch, R., 2013. An exploratory model study of sediment transport sources and deposits in the Bohai Sea, Yellow Sea, and East China Sea. *Journal of Geophysical Research: Oceans*, 118, 5908-5923.

Bohling, B., 2005. Estimating the risk for erosion of surface sediments in the Mecklenburg Bight (south-western Baltic Sea). *Baltica*, 18, 3-12.

Bobertz, B. and Harff, J., 2004. Sediment facies and hydrodynamic setting: a study in the south western Baltic Sea. *Ocean Dynamics*, 54, 39-48.

Chough, S. K.; Kim, J. W.; Lee, S. H.; Shinn, Y. J.; Jin, Y. J.; Suh, M. C., and Lee, J. S., 2002. High-resolution acoustic characteristics of epicontinental sea deposits, central-eastern Yellow Sea. *Marine Geology*, 188, 317-331.

Fang, G.; Wang, Y.; Wei, Z.; Choi, B. H.; Wang, X., and Wang, J., 2004. Empirical cotidal charts of the Bohai, Yellow, and East China Seas from 10 years of TOPEX/Poseidon altimetry. *Journal of Geophysical Research*, 109, C11006.

Fredsoe, J. and Deigaard, R., 1992. Mechanics of Coastal Sediment Transport. *World Scientific, Singapore.*

Grant, W. D. and Madsen, O. S., 1979. Combined wave and current interaction with a rough bottom. *Journal of Geophysical Research*, 84, 1797-1808.

Grass, A. J., 1970. Initial instability of fine bed sand. *Journal of Hydraulic Research*, 96, 619-632.

Harff, J. and Davis, J. C., 1990. Regionalization in Geology by multivariate classification. *Mathematical Geology*, 22, 925-936.

Hulscher, S. and Brink, van G. M., 2001. Comparison between predicted and observed sand waves and sand banks in the North Sea. *Journal of Geophysical Research*, 106, 9327-9338.

Jonsson, I. G. and Carlsen, N. A., 1976. Experimental and theoretical investigations in an oscillatory rough turbulent boundary layer. *Journal of Hydraulic Research*, 14, 45-60.

Kuhrts, C.; Fennel, W., and Seifert, T., 2004. Model studies of transport of sedimentary material in the western Baltic. *Journal of Marine Systems*, 52, 167-190.

Lavelle, J. W. and Mofjeld, H. O., 1987. Do critical stresses for incipient motion and erosion really exist? *Journal of Hydraulic Engineering*, 113, 370-385.

Li, C. X.; Zhang, J. Q.; Fan, D. D., and Deng, B., 2001. Holocene regression and the tidal radial sand ridge system formation in the Jiangsu coastal zone, east China. *Marine Geology*, 173, 97-120.

Li, G. X.; Chen, Z. G., and Liu, Y., 2005. *Sediment distribution map of the East China Sea.* Science Press, Beijing. Enclosure.

Liu, Z. X.; Xia, D. X.; Berne, S.; Wang, K. Y.; Marsset, T.; Tang, Y. X., and Bourillet, J. F., 1998. Tidal deposition systems of China's continental shelf, with special reference to the eastern BohaiSea. *Marine Geology*, 145, 225-253.

Lopez, F. and Garcia, M. H., 2001. Risk of sediment erosion and suspension in turbulent flow. *Journal of Hydraulic Engineering*, 127, 231-235.

Lu, J.; Qiao, F. L.; Wang, X. H.; Wang, Y. G.; Teng, Y., and Xia, C. S., 2011. A numerical study of transport dynamics and seasonal variability of the Yellow River sediment in the Bohai and Yellow seas. *Estuarine, Coastal and Shelf Science*, 95, 39-51.

Park, S. C. and Lee, S. D., 1994. Depositional patterns of sand ridges in tide-dominated shallow water environments: Yellow Sea coast and South Sea of Korea. *Marine Geology*, 120, 89-103.

Rijn, L., 2007. Unified view of sediment transport by current and waves. I: Initiation of motion, bed roughness and bed-load transport. *Journal of Hydraulic engineering*, 133, 649-667.

Shepard, F. P., 1954. Nomenclature based on sand-silt-clay ratios. *Journal of Sedimentary Petrology*, 24, 151-158.

Shi, X.; Liu, Y.; Chen, Z.; Wei, J.; Ge, S.; Wang, K.; Wang, G.; Yang, S.; Qiao, S.; Cai, D.; Cheng, Z.; Bu, W., and Li, H., 2012. Origin, transport process and distribution pattern of modern sediments in the Yellow Sea. *International Association of Sedimentologists, Special Publication*, 44, 321-350.

Smith, J. D. and McLean, S. R., 1977. Spatially averaged flow over a wavy bed. *Journal of Geophysical Research*, 82, 1735-1746.

Soulsby, R. L., 1997. *Dynamics of marine sands.* Telford Publ., London.

Styles, R. and Glenn, S. M., 2000. Modeling stratified wave and current bottom boundary layers on the continental shelf. *Journal of Geophysical Research*, 105, 24,119-24,139.

Swift, D. J. P., 1975. Tidal sand ridges and shoal-retreat massifs. *Marine Geology*, 18, 105-134.

Uehara, K.; Saito, Y., and Hori, K., 2002. Paleotidal regime in the Changjiang (Yangtze) Estuary, the East China Sea, and the Yellow Sea at 6 ka and 10 ka estimated from a numerical model. *Marine Geology*, 183, 179-192.

Veen, H. H.; Hulscher, S. J., and Knaapen, M. A., 2006. Grain size dependency in the occurence of sand waves. *Ocean Dynamics*, 56, 228-234.

Wang, Y.; Zhang, Y. Z.; Zou, X. Q.; Zhu, D., and Piper, D., 2012. The sand ridge field of the South Yellow Sea: origin by river-sea interaction. *Marine Geology*, 291-294, 132-146.

Wang, S. L.; Liu, J.; Li, W.; Zhou, L. Y.; Kong, X. H. and Liang, Y., 2006. A preliminary study on the tidal sand ridges offshore the Eastern Shandong Peninsula. *Marine Geology Letters*, 22, 1-5. (In Chinese with English abstract)

Wang, P.; Jia, K.; Wu, J. Z., and Hu, R. J., 2015. Distribution pattern of sand ridges and sand sheets in Bohai Sea and the relationship with M2 tidal current. *Marine Geology & Quaternary Geology*, 35, 23-32. (In Chinese with English abstract)

Xia, C.; Qiao, F.; Yang, Y.; Ma, J., and Yuan, Y., 2006. Three-dimensional structure of the summertime circulation in the Yellow Sea from a wave-tide circulation coupled model.

Journal of Geophysical Research, C11S03. 1–19. doi: 10.1029/2005JC003218.

Xing, F.; Wang, Y. P., and Wang, H. V. 2012. Tidal hydrodynamics and fine grained sediment transport on the radial sand ridge system in the southern Yellow Sea. *Marine Geology*, 291–294, 192–210.

Yang, C. S., 1989. Active, moribund and buried tidal sand ridges in the East Chna Sea andthe Southern Yellow Sea. *Marine Geology*, 88, 97–116.

Zhu, Y. and Chang, R., 2000. Preliminary study of the dynamic origin of the distribution pattern of bottom sediments on the continental shelves of the Bohai Sea, Yellow Sea and East China Sea. *Estuarine, Coastal and Shelf Science*, 51, 663–680.